

σ and ω meson propagation in a dense nuclear medium

K. Saito*

Physics Division, Tohoku College of Pharmacy

Sendai 981-8558, Japan

K. Tsushima[†], A.W. Thomas[‡] and A.G. Williams[§]

Special Research Center for the Subatomic Structure of Matter

and Department of Physics and Mathematical Physics

The University of Adelaide, SA 5005, Australia

*ksaito@nucl.phys.tohoku.ac.jp

†ktsushim@physics.adelaide.edu.au

‡athomas@physics.adelaide.edu.au

§awilliam@physics.adelaide.edu.au

Abstract

The propagation of the scalar (σ) and vector (ω) mesons in nuclear matter is studied in detail using the Walecka model over a wide range of densities and including the effects of a finite σ width through the inclusion of a two-pion loop. We calculate the dispersion relation and spectral functions of the σ and (transverse and longitudinal) ω mesons, including the effect of σ - ω mixing in matter. It is shown that the mixing effect is quite important in the propagation of the (longitudinal) ω and σ mesons above normal nuclear matter density. We find that there is a two-peak structure in the spectral function of the σ channel, caused by σ - ω mixing.

PACS numbers: 21.65.+f, 24.10.Jv, 21.30.Fe, 25.75.-q, 14.40.-n

Keywords: quantum hadrodynamics, dense nuclear matter, vector-scalar mixing, dispersion relation, spectral function

Recently much attention has been focussed on the variation of hadron properties in hot and/or dense nuclear matter[1]. In particular, the medium modification of the light vector (ρ , ω and ϕ) meson masses has been investigated by many authors[2, 3, 4, 5, 6, 7, 8, 9]. Experimentally, dilepton production in hot and/or dense nuclear matter produced by relativistic heavy ion collisions can provide a unique tool to measure such modifications. It is well known that data obtained at the CERN/SPS by the CERES[10] and HELIOS[11] collaborations show a significant amount of strength below the free ρ meson peak. Some authors[12] have concluded that this is caused by a downward shift of the rho meson mass in dense nuclear matter. To test this idea, measurements of the dilepton spectrum from vector mesons produced in nuclei are planned at TJNAF[13] and GSI[14] (see also Ref.[15]).

On the other hand, the σ meson has been treated as a correlated two-pion state in the scalar channel for a long time. However, recently some people have reanalysed the s-wave ($I=0$) $\pi\pi$ -scattering phase shift, and argued for the existence of the σ as a genuine resonance[16]. From the theoretical side, it is also anticipated that the σ meson may play an important role as the chiral partner of the π meson[17]. Some experimental possibilities have been proposed for investigating the behaviour of the σ in hot and/or dense nuclear matter[17, 18].

It is well known that in nuclear matter the σ can couple to the longitudinal mode of the ω meson[19]. This work is an extension and elaboration of studies in Ref.[3] where the invariant mass of the ω meson moving in nuclear matter was studied. Here, we generalize this work by including free space widths for the σ and ω and by studying σ - ω mixing in some detail as a function of density. Recently Wolf *et al.*[20] studied the effect of σ - ω mixing on the e^+e^- -pair production in relativistic heavy ion collisions. However they calculated only the lowest order mixing diagram, and did not include the nucleon-loop diagrams for the σ and ω meson propagators. The interesting results obtained in these earlier papers and the experimental relevance of the problem suggests that it is time for a more complete self-consistent calculation.

A complete investigation of the propagation of σ and ω mesons in a dense nuclear medium requires that one includes the effect of σ - ω mixing. In this letter we will study in detail the medium modification of σ and ω mesons in dense (symmetric) nuclear matter using the simplest version of quantum hadrodynamics (QHD or the Walecka model)[21] and including σ - ω mixing, $\sigma\pi\pi$ coupling, and the ω width.

The lagrangian density of the Walecka model (QHD-I) is well known and a full description of it can be found in Ref.[21]. We first treat the nuclear ground state in relativistic Hartree approximation (RHA), which is also explained in Ref.[21]. Here we shall ignore the coupling to the channels involving iso-vector mesons, neglecting, for example, $\omega + N \rightarrow \pi + N$ and $\omega + N \rightarrow \rho + N$ [22].

To compute the meson propagators, we sum over the ring diagrams, which consist of repeated insertions of the lowest order one-loop proper polarization part. This is the relativistic, random phase approximation (RPA)[19]. Since we want to include σ - ω mixing, it is convenient to use a meson propagator \mathcal{D}_{ab} in the form of a 5×5 matrix with indices a, b running from 0 to 4, where 4 is for the σ channel and $0 \sim 3$ are for the ω .

Dyson's equation for the full propagator, \mathcal{D} , is given in matrix form as:

$$\mathcal{D} = \mathcal{D}^0 + \mathcal{D}^0 \Pi \mathcal{D}, \quad (1)$$

where \mathcal{D}^0 is the lowest order meson propagator given by a block-diagonal form as

$$\mathcal{D}^0 = \begin{pmatrix} D_{\mu\nu}^0 & 0 \\ 0 & \Delta_0 \end{pmatrix}. \quad (2)$$

In Eq.(2) the noninteracting propagators for the σ and ω are given respectively by

$$\Delta_0(q) = \frac{1}{q_\mu^2 - m_\sigma^2 + i\epsilon}, \quad (3)$$

$$D_{\mu\nu}^0(q) = \frac{\xi_{\mu\nu}}{q_\mu^2 - m_\omega^2 + i\epsilon}, \quad (4)$$

where $\xi_{\mu\nu} = -g_{\mu\nu} + (q_\mu q_\nu / q_\mu^2)$, $q_\mu^2 = q_0^2 - |\vec{q}|^2$, and m_σ and m_ω are the free σ and ω meson masses.

The polarization insertion in Eq.(1) is also then given by a 5×5 matrix,

$$\Pi = \begin{pmatrix} \Pi_{\mu\nu}(q) & \Pi_\nu^m(q) \\ \Pi_\mu^m(q) & \Pi_s(q) \end{pmatrix}, \quad (5)$$

where the lowest order scalar, vector and scalar-vector-mixed polarization insertions are given respectively as

$$\Pi_s(q) = -ig_s^2 \int \frac{d^4k}{(2\pi)^4} \text{Tr}[G(k)G(k+q)] + \frac{3}{2}ig_{\sigma\pi}^2 m_\pi^2 \int \frac{d^4k}{(2\pi)^4} \Delta_\pi(k)\Delta_\pi(k+q), \quad (6)$$

$$\Pi_{\mu\nu}(q) = -ig_v^2 \int \frac{d^4k}{(2\pi)^4} \text{Tr}[G(k)\gamma_\mu G(k+q)\gamma_\nu], \quad (7)$$

$$\Pi_\mu^m(q) = ig_s g_v \int \frac{d^4k}{(2\pi)^4} \text{Tr}[G(k)\gamma_\mu G(k+q)]. \quad (8)$$

Note that we have added the contribution from the pion-loop to Π_s (the second term in the r.h.s. of Eq.(6)) in order to treat the σ more realistically. The pion propagator, Δ_π , is given by equation (3) with the pion mass m_π instead of m_σ . Here g_v , g_s and $g_{\sigma\pi}$ are respectively the nucleon- ω , nucleon- σ and σ - π coupling constants. We denote $G(k)$ as the self-consistent RHA nucleon propagator, which is given by the sum of the Feynman (F) part and the density-dependent (D) part as

$$\begin{aligned} G(k) &= G_F(k) + G_D(k), \\ &= (\gamma^\mu k_\mu^* + M^*) \left[\frac{1}{k_\mu^{*2} - M^{*2} + i\epsilon} + \frac{i\pi}{E_k^*} \delta(k_0^* - E_k^*) \theta(k_F - |\vec{k}|) \right], \end{aligned} \quad (9)$$

where $k^{*\mu} = (k^0 - g_v V^0, \vec{k})$ (V^0 is the mean value of the ω field), $E_k^* = \sqrt{\vec{k}^2 + M^{*2}}$ (M^* is the effective nucleon mass in matter) and k_F is the Fermi momentum. Therefore, each polarization insertion (except the pion-loop contribution) can be divided into two pieces: the Feynman (F) (or vacuum) part, which does not involve the $\theta(k_F - |\vec{k}|)$ term, and the density-dependent (D) part. The explicit expressions for the various components of D can be found in Ref.[23].

We can work out the F parts using the method of dimensional regularization to remove the divergence in the loop calculations. We show the results explicitly. For the σ , we must renormalize two terms: the nucleon-loop and pion-loop diagrams. For the nucleon-loop

contribution to the σ we introduce the usual counter terms to the lagrangian[21]

$$\delta\mathcal{L}_\sigma = \sum_{l=2}^4 \frac{\alpha_l}{l!} \sigma^l + \frac{\zeta}{2} (\partial\sigma)^2, \quad (10)$$

which includes quadratic, cubic, quartic and wavefunction renormalization. To get the ‘‘physical’’ properties of the σ meson in free space, we impose the following condition on the F part of the nucleon-loop diagram[24]:

$$\Pi_s^{N-loop}(q_\mu^2, M^* = M) = \frac{\partial}{\partial q_\mu^2} \Pi_s^{N-loop}(q_\mu^2, M^* = M) = 0 \quad \text{at } q_\mu^2 = m_\sigma^2, \quad (11)$$

where M is the free nucleon mass. We adjust the coefficients α_2 and ζ to satisfy this condition. For α_3 and α_4 we use the usual values given in Ref.[21]. For the pion-loop, we also introduce an appropriate counter term to the lagrangian, and require a similar condition to Eq.(11) for the polarization insertion of the pion-loop diagram in free space:

$$\Re e \Pi_s^{\pi-loop}(q_\mu^2) = 0 \quad \text{at } q_\mu^2 = m_\sigma^2. \quad (12)$$

Finally, we find

$$\begin{aligned} \Pi_s^{N-loop}(q) &= \frac{3g_s^2}{2\pi^2} \left[\frac{1}{6} (m_\sigma^2 - q_\mu^2) \right. \\ &\quad - \left(M^{*2} - \frac{q_\mu^2}{6} \right) \left(2 \ln \frac{M^*}{M} + f(x_q) - f(z_s) \right) \\ &\quad + \frac{q_\mu^2}{3} \left(\frac{M^{*2}}{q_\mu^2} (f(x_q) - 2) - \frac{M^2}{m_\sigma^2} (f(z_s) - 2) \right) \\ &\quad \left. - (M^{*2} - M^2)(f(z_s) - 2) + 2M(M^* - M) + 3(M^* - M)^2 \right], \end{aligned} \quad (13)$$

where $x_q = 1 - \frac{4M^{*2}}{q_\mu^2}$, $z_s = 1 - \frac{4M^2}{m_\sigma^2}$ and

$$\Pi_s^{\pi-loop}(q) = \frac{3g_{\sigma\pi}^2}{32\pi^2} m_\pi^2 [f(x_\pi) - \Re e f(z_\pi)], \quad (14)$$

where $x_\pi = 1 - \frac{4m_\pi^2}{q_\mu^2}$ and $z_\pi = 1 - \frac{4m_\pi^2}{m_\sigma^2}$, and

$$f(y) = \begin{cases} \sqrt{y} \ln \frac{\sqrt{y}+1}{\sqrt{y}-1}, & \text{for } 1 \leq y < +\infty \\ \sqrt{y} \ln \frac{1+\sqrt{y}}{1-\sqrt{y}} - i\pi\sqrt{y}, & \text{for } 0 < y < 1 \\ 2\sqrt{-y} \tan^{-1} \frac{1}{\sqrt{-y}}. & \text{for } y \leq 0 \end{cases} \quad (15)$$

For the ω , we add the counter term for the wavefunction renormalization to the lagrangian and require the following condition for the F part of the polarization insertion of the nucleon-loop:

$$\Pi_{\mu\nu}^{N-loop}(q) = \xi_{\mu\nu}\Pi^{N-loop}(q_\mu^2, M^* = M) = 0 \quad \text{at } q_\mu^2 = m_\omega^2. \quad (16)$$

Then, we get

$$\begin{aligned} \Pi^{N-loop}(q) &= \frac{g_v^2}{6\pi^2} q_\mu^2 \left[2 \ln \frac{M^*}{M} - 4 \left(\frac{M^{*2}}{q_\mu^2} - \frac{M^2}{m_\omega^2} \right) \right. \\ &\quad \left. + \left(1 + 2 \frac{M^{*2}}{q_\mu^2} \right) f(x_q) - \left(1 + 2 \frac{M^2}{m_\omega^2} \right) f(z_v) \right], \end{aligned} \quad (17)$$

where $z_v = 1 - \frac{4M^2}{m_\omega^2}$. Note that vacuum fluctuations do not contribute to the mixed part of Eq.(8).

Using these polarization insertions, we define the dielectric function ϵ as[19, 21, 23]

$$\begin{aligned} \epsilon &= \det(1 - \mathcal{D}^0\Pi), \\ &= \epsilon_T^2 \times \epsilon_{SL}, \end{aligned} \quad (18)$$

where $\epsilon_{T[SL]}$ is the dielectric function for the transverse (T) [scalar and longitudinal (SL)] mode. (Note that the full propagator Eq.(1) can be rewritten as $\mathcal{D} = \mathcal{D}^0/(1 - \mathcal{D}^0\Pi)$ and hence $\det\mathcal{D} = \det\mathcal{D}^0/\epsilon$.) Then, we find

$$\epsilon_T = 1 - d_0\Pi_T, \quad (19)$$

$$\epsilon_{SL} = (1 - d_0\Pi_L)(1 - \Delta_0\Pi_s) - \frac{q_\mu^2}{q^2} \Delta_0 d_0 (\Pi_0^m)^2. \quad (20)$$

Here $q = |\vec{q}|$ and $d_0^{-1} = q_\mu^2 - m_\omega^2 + im_\omega\Gamma_\omega^0$, where we add the width of the ω in free space ($\Gamma_\omega^0 = 9.8$ MeV). The transverse (Π_T) and longitudinal (Π_L) components of the polarization insertion Eq.(7) are respectively defined by Π_{11} (or Π_{22}) and $\Pi_{33} - \Pi_{00}$ (we choose the direction of \vec{q} as the z -axis). Note that Π_0^m is the 0-th component of the mixed polarization insertion Eq.(8), which vanishes when $q = 0$ (because of current conservation). The eigencondition for determining the collective excitation spectrum is just equivalent to searching for the zeros of the dielectric functions. Since we are interested in the medium

modification of the meson propagation, we restrict ourselves here to the meson branch in the time-like region.

To study the dispersion relation of the meson branch, we first have to solve the nuclear ground state within RHA. Because we choose α_2 and ζ to satisfy the renormalization condition for the σ at $q_\mu^2 = m_\sigma^2$ (see Eq.(11)), the total energy density is written as

$$\mathcal{E} = \mathcal{E}_0 + \frac{1}{2\pi^2} M^2 (M - M^*)^2 \left[\frac{m_\sigma^2}{4M^2} + \frac{3}{2} f(z_s) - 3 \right], \quad (21)$$

where \mathcal{E}_0 is the usual one (in RHA) given in Ref.[21]. (Note that in Ref.[21] the renormalization condition on nucleon loops is imposed at $q_\mu^2=0$. This difference yields the second term of the r.h.s. of Eq.(21)[24]. As a result, our model gives the same physical quantities as those of Ref.[21].) Requiring the saturation condition, $\mathcal{E}/\rho_B - M = -15.7$ MeV at $\rho_0 = 0.15 \text{ fm}^{-3}$ (where ρ_B and ρ_0 are respectively the density of nuclear matter and the saturation density), we determine the coupling constants g_s^2 and g_v^2 : $g_s^2 = 101.50$ and $g_v^2 = 72.296$. In the calculation we fix the values of the free hadron masses to be $M = 939$ MeV, $m_\sigma = 550$ MeV, $m_\omega = 783$ MeV and $m_\pi = 138$ MeV. This yields the effective nucleon mass $M^*/M = 0.73$ at ρ_0 and the incompressibility $K = 452$ MeV. We do not consider the possibility of medium modification of the pion loop or any of the coupling constants in the present work.

To determine the coupling constant $g_{\sigma\pi}$, we adjust it to fix the width of the σ in free space. Since the full propagator of σ in free space is given in terms of the pion-loop polarization insertion, the width Γ_σ^0 is given by

$$\Gamma_\sigma^0 = -\frac{\Im m \Pi_s^{\pi-loop}}{m_\sigma} \quad \text{at } q_\mu^2 = m_\sigma^2. \quad (22)$$

If we choose $\Gamma_\sigma^0 = 300$ MeV[16], we find $g_{\sigma\pi} = 18.33$.

Now we are in a position to show our results. First, in Fig. 1, we show the dispersion relation for the meson branches, which are calculated by searching for the zeros of the real part of the dielectric function given in Eq.(20). As illustrated in the figure, if the σ - ω mixing is ignored, the longitudinal (L) mode and the σ (S) mode cross each other at one point. However, once the mixing is involved, the two modes *never* cross each other.

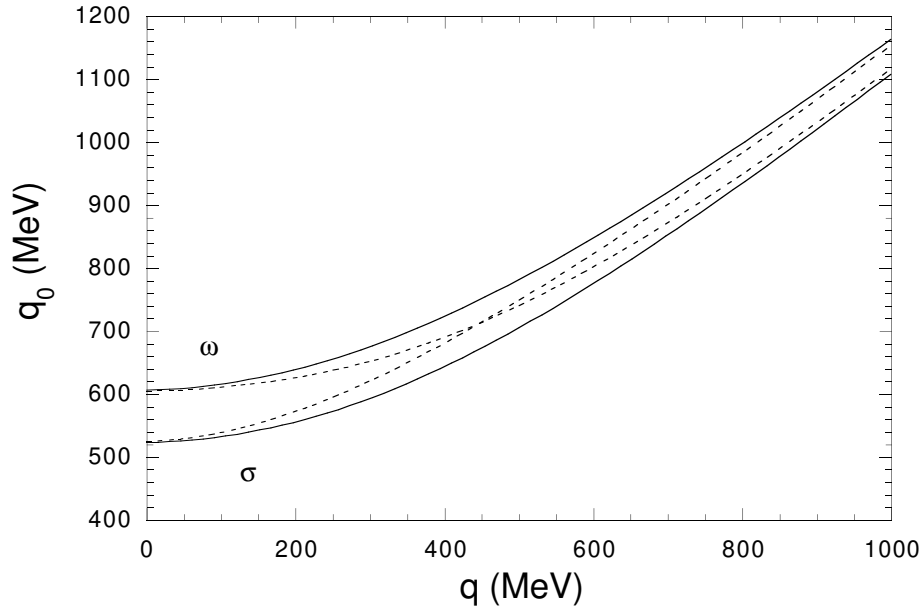


Figure 1: Dispersion relation for the scalar and longitudinal modes at $\rho_B/\rho_0 = 2$. The curves specified by ω are for the longitudinal component of the ω meson. The dotted curves are the results without σ - ω mixing. The solid curves include the effect of mixing. (Note that the transverse mode is very close to the upper solid curve.)

We can understand this phenomenon as a level-level repulsion due to the mixing, which is quite familiar in conventional nuclear physics, for example, in the Nilsson diagram (see Ref.[25]). Adding the off-diagonal (or mixing) matrix element in the Hamiltonian leads to new eigenstates which never cross each other. The new states approach the original crossing modes as the off-diagonal part becomes weaker. This occurs at mid and high density (above $\sim \rho_0$) because its origin is the mixing effect, which vanishes at $\rho_B = 0$.

In Figs. 2 and 3, we show the “invariant mass” ($m_{inv}^* \equiv \sqrt{q_0^2 - q^2}$, with q_0 chosen as in Fig. 1 so that the real part of the dielectric function vanishes for that value of q) as a function of density. As shown in the figures, we can clearly see the role of mixing, which is quite important in determining the meson mass at mid and high density. If the mixing is ignored, the masses of the L and S modes cross each other, like the dispersion relation shown in Fig. 1, and the L mass is below the other two at high density. However, in the

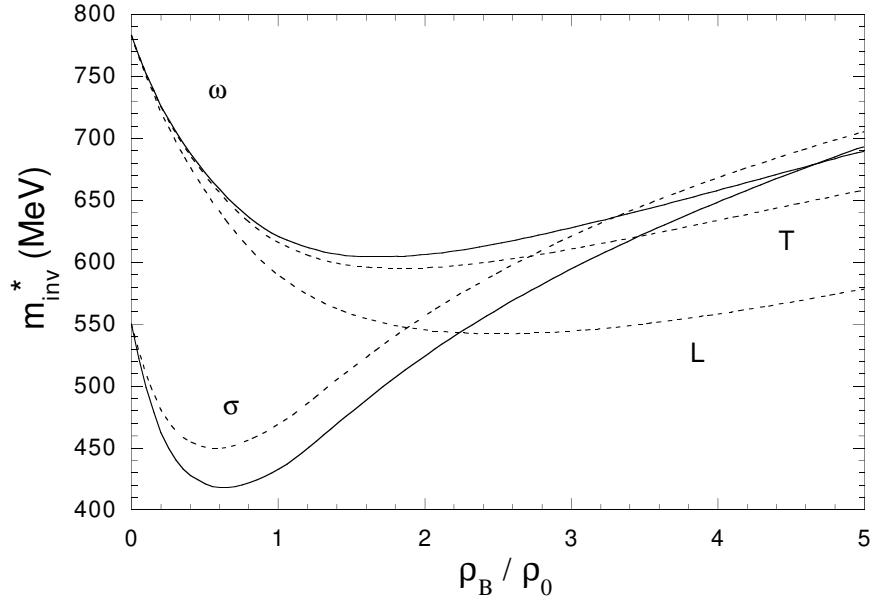


Figure 2: “Invariant mass” without σ - ω mixing. The solid curves are for three-momentum transfer $q=1$ MeV. The L and T modes of the ω are almost degenerate. The dotted curves are for $q=500$ MeV, in which case the L and T modes are well separated.

case where the mixing is included the L and S masses never cross each other. At high density the L mass is pushed upwards, while the S mass is pulled downwards because of mixing (through the level-level repulsion). From the figures we can see that the mixing effect becomes vital above $\sim \rho_0$.

Next we calculate the spectral functions of the T, L and S modes. It is very interesting to study these functions because in a thermal model the dilepton yields in heavy ion collisions would be proportional to the spectral functions. The spectral function is usually defined in terms of the imaginary part of the full propagator. For the T mode it is:

$$S_T(m_{inv}^*, q, \rho_B) = -\frac{1}{\pi} \Im m \left[\frac{d_0}{1 - d_0 \Pi_T} \right]. \quad (23)$$

While, in practice, it may be difficult or even impossible to separate the L and S modes in an experiment, it is of considerable theoretical interest to study the following spectral

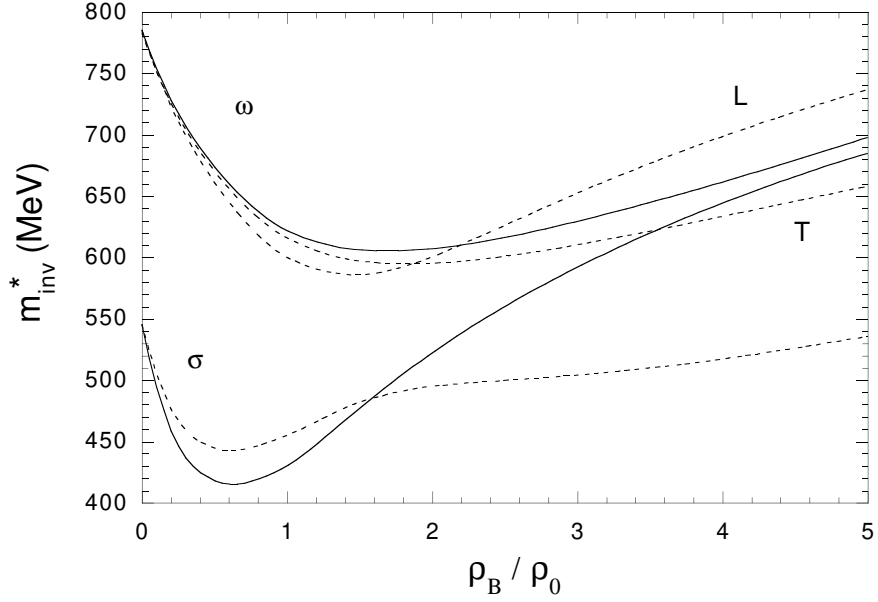


Figure 3: “Invariant mass” including σ - ω mixing. The solid curves are for $q=1$ MeV. The L and T modes of the ω are again very close to each other. The dotted curves are for $q=500$ MeV.

functions:

$$S_L(m_{inv}^*, q, \rho_B) = -\frac{1}{\pi} \Im m \left[\frac{d_0(1 - \Delta_0 \Pi_s)}{\epsilon_{SL}} \right], \quad (24)$$

$$S_S(m_{inv}^*, q, \rho_B) = -\frac{1}{\pi} \Im m \left[\frac{\Delta_0(1 - d_0 \Pi_L)}{\epsilon_{SL}} \right], \quad (25)$$

corresponding to the complete, diagonal, longitudinal ω and σ propagators, respectively.

In Figs. 4, 5 and 6, we show the shape of the spectral function S_i ($i=T, L$ or S), as a function of the invariant mass and three-momentum transfer, at $\rho_B/\rho_0=2$. For the T mode the shape is very simple, while for the L and S modes they are complicated because of the effect of mixing. In particular, the S mode is quite remarkable: at $q=0$ MeV there is only one peak, while at fixed, finite q there exist *two peaks* in the spectral function. Note that at $q=0$ MeV the mixed polarization insertion vanishes, so this two-peak structure is clearly associated with σ - ω mixing. As the density grows the two peaks becomes separated more widely. In the L mode there is no such structure at fixed q . However, the peak at

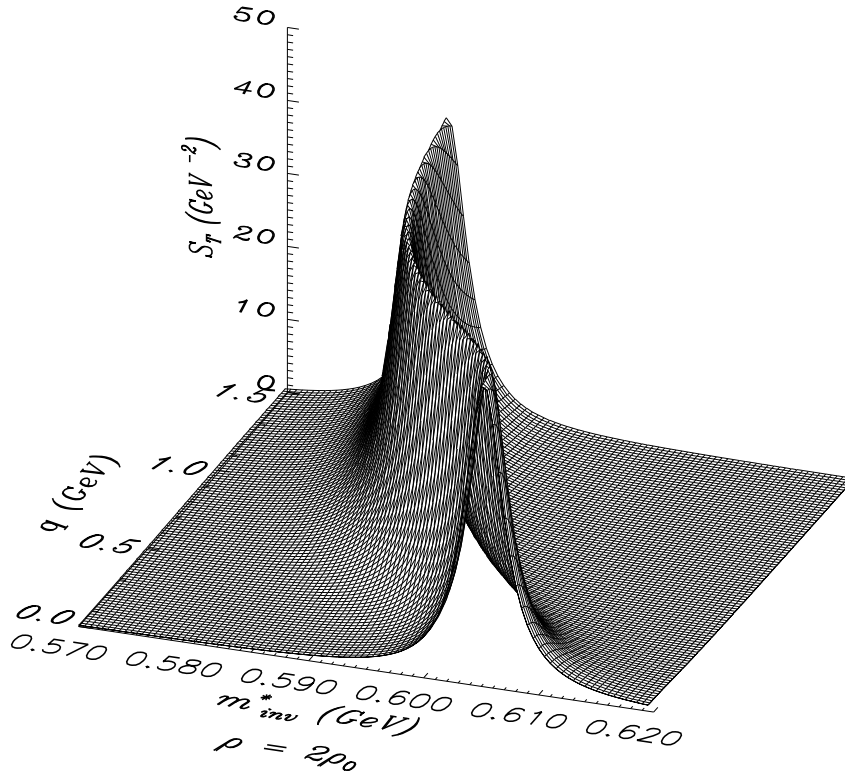


Figure 4: Spectral function for the transverse ω at $\rho_B/\rho_0 = 2$.

low q and that at high q are separated very well and the values of their invariant masses are quite different. As the density goes up this tendency becomes more clear.

Finally, we should comment on the width of the σ in free space. In our calculation we have used $\Gamma_\sigma^0 = 300$ MeV[16] (see Eq.(22)), which is somewhat smaller than usual. We have therefore also calculated the spectral functions using a width of 600 MeV but, as the results were not qualitatively different we do not report them here.

In summary, we have studied the propagation of σ and ω mesons and the effect of σ - ω mixing in dense (symmetric) nuclear matter, within the Walecka model. We have illustrated that the effect of mixing is quite important in the propagation of the longitudinal ω and σ mesons at a density above $\sim \rho_0$. In the scalar (or σ) channel we have found a two-peak structure in the spectral function at finite three-momentum transfer,

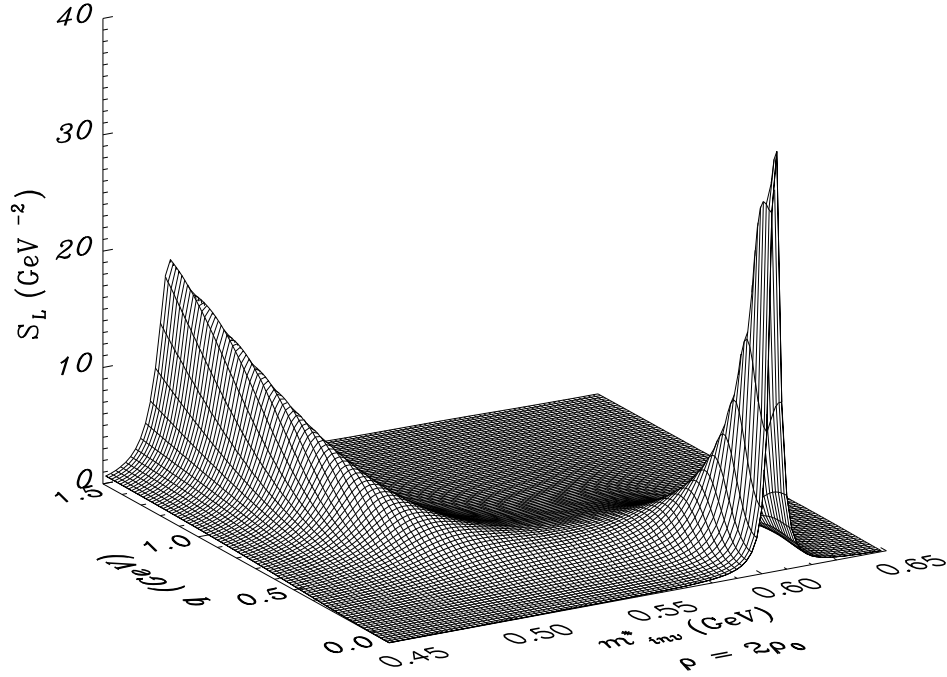


Figure 5: Spectral function for the longitudinal ω at $\rho_B/\rho_0 = 2$.

which could be measured in future experiments[18]. It would clearly be very interesting to compare these results with the medium modification of the meson propagation using the quark-meson coupling (QMC) model[7], in which the effect of hadron internal structure is involved. We will report such a study in the near future.

This work was supported by the Australian Research Council, and the Japan Society for the Promotion of Science.

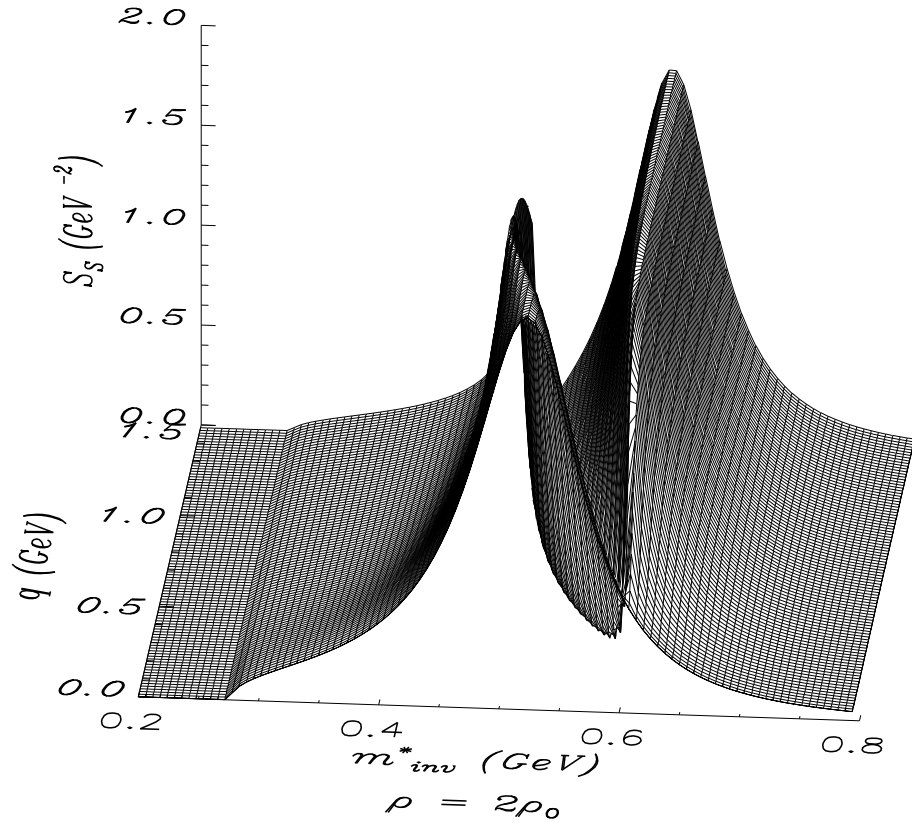


Figure 6: Spectral function for the σ at $\rho_B/\rho_0 = 2$.

References

- [1] Quark Matter '97, to be published in Nucl. Phys. A (1998).
- [2] K. Saito, T. Maruyama and K. Soutome, Phys. Rev. C40, 407 (1989);
J.C. Caillon and J. Labarsouque, Phys. Lett. B311, 19 (1993);
T. Hatsuda, H. Shiomi and H. Kuwabara, Prog. Thor. Phys. 95, 1009 (1996).
- [3] H.-C. Jean, J. Piekarewicz and A.G. Williams, Phys. Rev. C49, 1981 (1994).
- [4] G.E. Brown and M. Rho, Phys. Rev. Lett. 66, 2720 (1991)
- [5] M. Asakawa, C.M. Ko, P. Lévai and X.J. Qiu, Phys. Rev. C46, R1159 (1992);
M. Asakawa and C.M. Ko, Phys. Rev. C48, R526 (1993).
- [6] T. Hatsuda and Su H. Lee, Phys. Rev. C46, R34 (1993);
F. Klingl, N. Kaiser and W. Weise, Nucl. Phys. A624, 527 (1997);
Su H. Lee, Phys. Rev. C57, 927 (1998).
- [7] K. Saito, K. Tsushima and A.W. Thomas, Phys. Rev. C 55, 2637 (1997); *ibid.* C 56, 566 (1997).
- [8] B. Friman, preprint GSI-98-7 (nucl-th/9801053).
- [9] For recent papers, see also
W. Peters, M. Post, H. Lenske, S. Leupold and U. Mosel, preprint UGI-97-09 (nucl-th/9708004);
L.A. Kondratyuk, A. Sibirtsev, W. Cassing, Ye.S. Golubeva and M. Effenberger, preprint UGI-97-04 (nucl-th/9801055);
J. Wambach and R. Rapp, preprint SUNY-NTG-98-03 (nucl-th/9802001);
F. Klingl and W. Weise, talk at the XXXVI Int. Winter Meeting on Nuclear Physics (hep-ph/9802211).
- [10] P. Wurm for the CERES collaboration, Nucl. Phys. A590, 103c (1995).

- [11] M. Masera for the HELIOS collaboration, Nucl. Phys. A590, 93c (1995).
- [12] G.Q. Li, C.M. Ko and G.E. Brown, Nucl. Phys. A606, 568 (1996);
G. Chanfray and R. Rapp and J. Wambach, Phys. Rev. Lett. 76, 368 (1996).
- [13] M. Kossov *et al.*, TJNAF proposal No. PR-94-002 (1994);
See also, P.Y. Bertin and P.A.M. Guichon, Phys. Rev. C42, 1133 (1990).
- [14] HADES proposal, see HADES home page: <http://piggy.physik.uni-giessen.de/hades/>
- [15] G.J. Lolos *et al.*, Phys. Rev. Lett. 80, 241 (1998).
- [16] N.A. Törnqvist and M. Roos, Phys. Rev. Lett. 76, 1575 (1996);
M. Harada, F. Sannino and J. Schechter, Phys. Rev. D54, 1991 (1996); Phys. Rev. Lett. 78, 1603 (1997);
S. Ishida *et al.*, Prog. Theor. Phys. 98, 1005 (1997).
- [17] T. Hatsuda and T. Kunihiro, Phys. Rep. 247, 221 (1994);
T. Kunihiro, preprint RYUTHP 97/3 (hep-ph/9710320).
- [18] H.A. Weldon, Phys. Lett. B274, 133 (1992);
S. Chiku and T. Hatsuda, preprint UTHEP-379 (hep-ph/9803226);
T. Kunihiro, Prog. Theor. Phys. Suppl. 120, 75 (1995);
T. Kunihiro, H. Shimizu and T. Hatsuda, private communication.
- [19] S.A. Chin, Ann. of Phys. 108, 301 (1977).
- [20] G. Wolf, B. Friman and M. Soyeur, preprint GSI-97-37 (nucl-th/9707055).
- [21] B.D. Serot and J.D. Walecka, Adv. Nucl. Phys. 16, 1 (1986).
- [22] The enhancement of the ω width due to the πN channel in nuclear matter is expected to be rather small, for example, ~ 30 MeV at normal nuclear matter density (see Ref.[8]).

- [23] K. Lim and C.J. Horowitz, Nucl. Phys. A501, 729 (1989). In the appendix there is one typo in the imaginary part of the transverse polarization insertion for the ω . The overall sign should be positive (C.J. Horowitz, private communication).
- [24] H. Kurasawa and T. Suzuki, Nucl. Phys. A490, 571 (1988).
- [25] W. Greiner and J.A. Maruhn, Nuclear Models, Springer (1996).